Jour. Korean Earth Science Society, v. 22, no. 4, p. 278-291, August 2001

Mesothermal Gold Vein Mineralization of the Seolhwa Mine: Fluid Inclusion and Sulfur Isotope Studies

Chul-Ho Heo[1,*] · Seong-Taek Yun[1] · Chil-Sup So[1] · Seon-Gyu Choi[1] Sang-Hoon Choi[2]

[1]Department of Earth and Environmental Sciences, Korea University, Seoul 136-701, Korea
[2]Department of Earth and Environmental Sciences, Chungbuk National University, Cheongju 361-763, Korea

설화 광산의 중열수 금광화작용: 유체포유물 및 황동위원소 연구

허철호[1,*] · 윤성택[1] · 소칠섭[1] · 최선규[1] · 최상훈[2]

[1]고려대학교 지구환경과학과, 136-701 서울특별시 성북구 안암동 5가 1
[2]충북대학교 지구환경과학과, 361-763 충북 청주시 흥덕구 개신동 산 48

Abstracts: Mesothermal gold vein minerals of the Seolhwa mine were deposited in a single stage of massive quartz veins which filled the mainly NE-trending fault shear zones exclusively in the granitoid of the Gyeonggi Massif. The Seolhwa mesothermal gold mineralization is spatially associated with the Jurassic granitoid of 161 Ma. The vein quartz contains three main types of fluid inclusions at 25°C: 1) low-salinity (< 5 wt.% NaCl), liquid CO_2-bearing, type IV inclusion; 2) gas-rich (> 70 vol.%), aqueous type II inclusions; 3) aqueous type I inclusions (0 ~ 15 wt.% NaCl) containing small amounts of CO_2. The H_2O-CO_2-CH_4-N_2-NaCl inclusions represent immiscible fluids trapped earlier along the solvus curve at temperatures from 430° to 250°C and pressures of 1 kbars. Detailed fluid inclusion chronologies may suggest a progressive decrease in pressure during the auriferous mineralization. The aqueous inclusion fluids represent either later fluids evolved through extensive fluid unmixing (CO_2-CH_4 effervescence) from a homogeneous H_2O-CO_2-CH_4-N_2-NaCl fluid due to decreases in temperature and pressure, or the influence of deep circulated meteoric waters possibly related to uplift and unloading of the mineralizing suites. The initial fluids were homogeneous containing H_2O-CO_2-CH_4-N_2-NaCl components and the following properties: the initital temperature of > 250° to 430°C, X_{CO_2} of 0.16 to 0.62, 5 to 14 mole% CH_4, 0.06 to 0.3 mole% N_2 and salinities of 0.4 to 4.9 wt.% NaCl. The T-X data for the Seolhwa gold mine may suggest that the Seolhwa auriferous hydrothermal system has been probably originated from the adjacent granitic melt which facilitated the CH_4 formation and resulted in a reduced fluid state evidenced by the predominance of pyrrhotite. The dominance of negative $\delta^{34}S$ values of sulfides (–0.6 to 1.4‰) are consistent with their deep igneous source.

Key words: mesothermal gold mineralization, fluid inclusion, sulfur isotope

요 약: 설화 광산의 중열수(中熱水) 금광상은 경기육괴의 화강암류내에 발달된 북동방향 단층 전단대를 충진한 괴상의 단성 석영맥내에 배태되어 있다. 설화 중열수 금광화작용(金鑛化作用)은 쥬라기 화강암류(161Ma)와 공간적으로 관련되어 있다. 맥상 석영은 3개유형의 유체포유물(流體包有物)을 포함하고 있다: 1) 저염농도(< 5wt.% NaCl)의 액상 CO_2를 배태한 type IV 유체포유물; 2) 가스가 풍부(>70vol.%)하고, 기상으로 균질화하는 type II 유체포유물; 3) 소량의 CO_2를 포함하는 저내지 중염농도(0 ~ 15 wt.% NaCl)의 type I 유체포유물. H_2O-CO_2-CH_4-N_2-NaCl계 유체포유물은 250° ~ 430°C 온도와 1kbar 압력에 해당되는 액상선을 따라 초기에 포획된 불혼화 유체를 지시한다. 정밀 유체포유물 연구에 의하면, 함금 광화작용중 점진적인 압력감소가 발생했음을 알 수 있다. 수용성 포유물의 유체는 온도 및 압력감소로 인한 균질한 H_2O-CO_2-CH_4-N_2-NaCl계 유체로부터 광역적인 유체의 불혼화(CO_2-CH_4 비등)작용을 거쳐 진화된 후기 유체이거나, 광화지역의 융기 및 삭박과 관련된 심부순환천수의 영향을 받았던 것으로 추정된다. 초기 유체는 균질한 H_2O-CO_2-CH_4-N_2-NaCl계 유체로서 다음과 같은 특성을 보인다: > 250° ~ 430°C, 0.16 ~ 0.62의 X_{CO_2}, 5 ~ 14 mole% CH_4,

*E-mail: chheo@mail.korea.ac.kr

0.06 ~ 0.31mole% N_2, 0.4 ~ 4.9wt.% NaCl의 염농도. 설화 금광산의 온도-조성 자료는 설화 함금열수계가 화강암질 용융체와 인접한 부분에 정치되어 있었음을 지시한다. 이러한 화강암질 용융체는 CH_4 형성을 촉진시켜 유체를 환원상태로 변환시킨 것으로 추정된다. 철황화물중 자류철석이 지배적으로 산출됨은 환원유체 상태를 지시하고 있다. 황화광물의 $\delta^{34}S$값(-0.6 ~ 1.4‰)은 황의 심부 화성기원을 지시하고 있다.

주요어: 중열수, 금광화작용, 유체포유물, 황동위원소

INTRODUCTION

Most gold-silver vein deposits in South Korea are associated intimately with major periods of Jurassic (Daebo series) and Cretaceous (Bulgugsa series) granitism (Shimazaki *et al.*, 1986). Three main types of Au-Ag deposits in Korea which display consistent relationships among mineralization age, depth, water to rock ratio, and Au/Ag ratio have been previously documented (Shelton *et al.*, 1988): gold-rich, mesothermal-type deposits (Jurassic), "Korean-type" gold-silver deposits (Early Cretaceous), and silver-rich, epithermal-type deposits (Late Cretaceous). Among these, mesothermal-type deposits are extremely rare in South Korea, and little is known about their genesis and ore fluid characteristics. The Seolhwa gold mine, which is located about 100 km south of Seoul (latitude 36° 43', longitude 127° 02' E) (Fig. 1), is one of the most important gold producers in South Korea. The mine was exploited until 1987, but is now closed. Ores at Seolhwa mine are emplaced within a series of fissure-filling hydrothermal quartz veins which are massive and mineralogically simple. In this paper, we document the nature and physicochemical conditions of gold mineralization in the Seolhwa mine using the fluid inclusion and sulfur isotope data.

GEOLOGY AND ORE VEINS

The geology of mine area consists of Precambrian banded biotite gneiss, Jurassic biotite granite, and acidic dyke (Fig. 1). The Precambrian banded biotite gneisses mainly consisting of quartz, plagioclase, biotite and orthoclase is distributed in the southern and north-eastern parts of the study area. The accessory minerals are garnet, sericite, sillimanite, chlorite, zircon, magnetite and epidote. Schistosity of the gneiss is clearly shown and its predomonant strike is N70° ~ 80° W and 60° ~ 65° SW dip. The main ore deposit is contained of biotite granite intruded by later acidic dyke throughout the mine district. The biotite granite with grayish white or pinkish gray tint contains quartz, feldspar and biotite with small amounts of amphibole and chlorite as the accessory minerals. It is characterized by fine- or medium grained equigranular texture and distributed around the Seolhwa Mountain. The Seolhwa biotite granite yields whole-rock Rb-Sr ages of 16±14 Ma (Heo *et al.*, 2001), corresponding a Late Jurassic age. In the southern parts of the mine district, granite porphyry whose size is too small to be shown in a geologic map, is partially distributed. It shows porphyroblastic texture containing the porphyroblasts of quartz and feldspar. Acidic dyke intruding biotite granite is silicic showing the width from 0.3 to 0.5 m. Joints developed in this area show the attitude which principally strikes N10° E and dips 68° NW.

The host rock of the deposit is biotite granite whose fissure is filled by a gold-bearing quartz vein. The vein strikes N10° ~ 20° E and dips 55 ~ 60° NW (Fig. 1). Vein width ranges from 0.05 to 0.1 m with relatively high grade. Ore grades range from 5.6 ~ 102.7 g/t Au and 3 ~ 17 g/t Ag (KORES, 1983). Electrum-base metal sulfide mineralization at the Seolhwa mine occurs in stages of massive quartz veins which are mineralogically simple. The veins contain minor amounts (usually < 5 vol.%) of ore minerals including molybdenite, scheelite, pyrite, marcasite, pyrrhotite, sphalerite, chalcopyrite, galena, tellurobismuthite, bismuthinite, native gold, and elec-

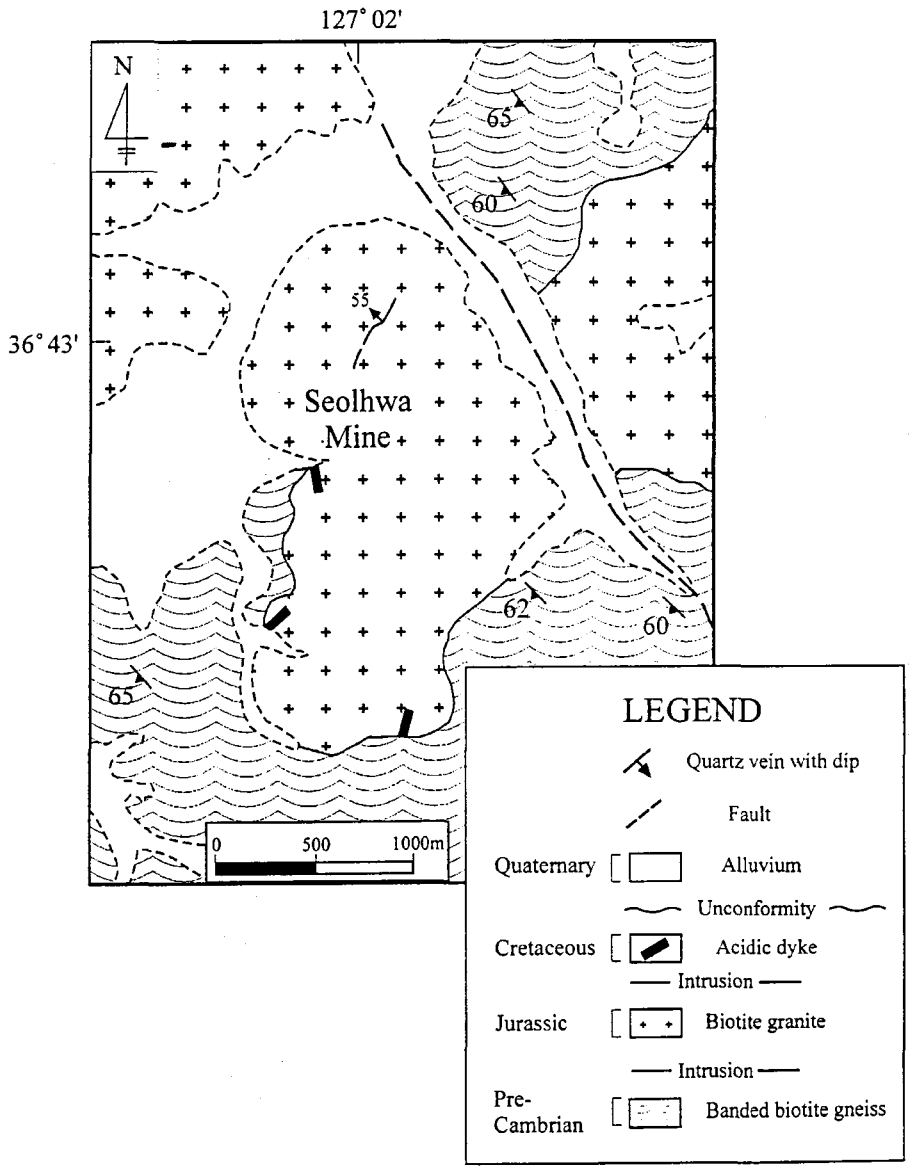

Fig. 1. Geologic map of the Seolhwa gold mine district.

trum. Wall-rock alteration occurs as narrow (< 0.4 m wide) linear zones adjacent to vein margins, bleaching the rocks green or white.

MINERALOGY AND PARAGENESIS

Veins of the Seolhwa gold mine were formed during two stages separated by a major tectonic fracturing events (Fig. 2): I. a quartz-sulfide-gold stage, II. a postore carbonate stage. Economic quantities of gold, together with quartz and sulfides, were introduced during stage I. Stage I mineralization is characterized by massive quartz containing sulfides. Massive quartz is frequently cut by randomly oriented fractures (mostly < 1 mm in width). These fratures are related to mineralization of later quartz, suggesting some fracturing events were contemporaneous with vein emplacements. Molybdenite, the early sulfide phase, occurs mainly as disseminations in veins and greisenized wall rocks. Scheelite

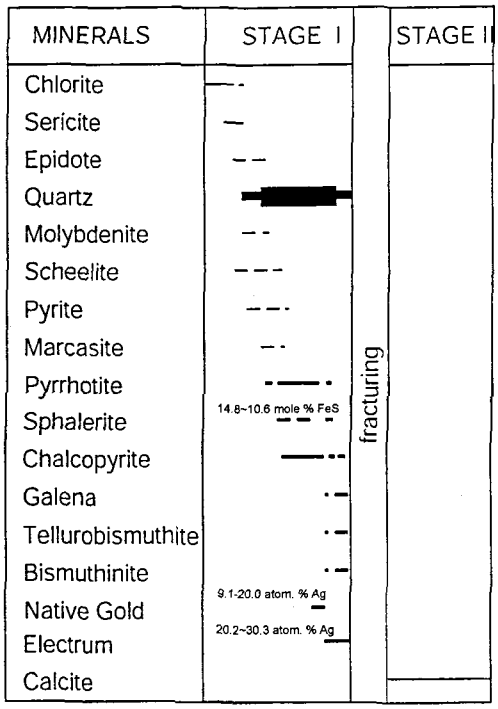

Fig. 2. Generalized paragenetic sequence of minerals from veins and alteration zones of the Seolhwa gold mine district.

occurs as anhedral masses intimately intergrown with chalcopyrite, pyrrhotite and sphalerite. Pyrite occurs as both wall-rock alteration products and fine euhedral to subhedral grains within quartz matrix. Pyrrhotite occurs as anhedral masses intergrown with chalcopyrite, scheelite, sphalerite, bismuthinite and chalcopyrite. Sphalerite occurs throughout the veins. Fine- to medium-grained sphalerites are rarely impregnated into the silicified wall-rock adjacent to the vein margins, forming dispersed euhedral to subhedral grains. Sphalerite (10.6 ~ 14.8 mole% FeS, Fig. 2) usually occurs as anhedral masses throughout the veins and is closely intergrown wth pyrrhotite and chalcopyrite. Lesser amounts of sphalerites occur within microfractures cutting quartz and sulfides, and they are associated with late quartz, chalcopyrite, and electrum. The late stage I mineralization is characterized by deposition of tellurobismuthite and bismuthinite. These minerals occur with electrum (20.2 ~ 30.3 atom.% Ag, Fig. 2) at central vein portions where galena is disseminated. Tellurobismuthite also occurs along small, galena-rich fractures cutting earlier vein materials. Bismuthinite occurs with chalcopyrite and pyrrhotite and intergrows with electrum. These Bi mineral and telluride are typically disseminated within anhedral galena as tiny (mostly < 10 μm) inclusions. Native gold (9.1 ~ 20.0 atom.% Ag, Fig. 2) occurs as free gold grains within the fracture of quartz and is intergrown with chalcopyrite. Electrum (20.2 ~ 30.3 atom.% Ag, Fig. 2) is frequently associated with bismuthinite, chalcopyrite, galena, sphalerite, and tellurobismuthite infilling fractures of quartz and sulfides.

FLUID INCLUSION STUDY

Vein mineral samples collected from Seolhwa gold mine were investigated by microthermometry in order to document the ranges of fluid compositions and temperatures during mineralization and to investigate thermal histories of auriferous hydrothermal fluids. Forty-five samples from the Seolhwa gold mine were collected within the vein quartz and some calcite. Sphalerites were not suitable for the study due to their opacity and massive occurrence. Microthermometric data were obtained on a U.S.G.S./Fluid Inc. gas-flow heating/freezing stage calibrated with synthetic H_2O and CO_2 inclusions and various organic solvents (Hollister, 1981; Shepherd *et al.*, 1985). Heating rates were varied but were maintained 1°C/min for determinations of melting temperatures and carbonaceous-phase homogenization temperatures and about 10°C/min for measurement of total homogenization temperatures. During freezing experiments, the sequential repeated freezing technique described by Haynes (1985) was employed over the expected temperatures in order to make phases coarsen to observable dimensions for optimum precision. Temperatures of total homogenization and carbonaceous-phase homogenization and melting temperatures of carbonaceous phase, ice and clathrate have standard errors of ±1.0° and ±0.2°C, respectively. The measured number of fluid

inclusion data is 618.

Occurrence and Types of Fluid Inclusions

Massive vein quartz from the Seolhwa gold deposit was inclusion-laden, probably due to repeated fracturing and healing both during and after quartz deposition. The size of fluid inclusions ranged from 3 to 27 μm (number of measurements = 618, avg. = 11). Three main types of fluid inclusions were identified based on their appearance at room temperature, combined with their behavior during cooling down to about −100°C and slight heating up to about 30°C (Nash, 1972). They have been grouped into three types according to room temperature phase behavior (Fig. 3): type I, type II, and type IV inclusions. Two subtypes of type I fluid inclusions have been distinguished on the basis of their occurrence and compositional characteristics: type Ia (primary and/or pseudosecondary aqueous fluid inclusions showing the presence of a nucleated clathrate upon heating after cooling) and type Ib (aqueous inclusions). Type IV inclusions are subdivided into two types: type IVa (homogenized into aqueous phase) and type IVb (homogenized into carbonaceous phase) upon slight heating (up to about 30°C). All types (Type I, II and IV) of fluid inclusions have been observed in stage I vein quartz. Stage II calcite samples contain type Ib inclusions only.

Type I inclusions: These fluid inclusions consist of two phases (H_2O-rich, liquid and vapor) at room temperatures. Type Ia inclusins are generally tabular or negative-shaped, and their gas bubble comprises 10 to 45 percent of the total inclusion volume. Type Ia inclusions contain minor amounts of CO_2, recognized during the microthermometry. The occurrence modes of type Ia inclusions are summarized as follows: (1) isolated inclusions in regular-shaped vacuoles distributed randomly; (2) trails of inclusions commonly representing healed fractures relevant to gold-containing quartz veinlets. According to Roedder (1981 and 1984), mode (1) indicates a primary origin, whereas mode (2) reflects a pseudosecondary origin. The occurrences of type Ib inclusions (less than 15 vol.%, mostly < 5% of gas) are as follows: 1) inclusions are parallel to growth zone or crystal faces, indicating a primary origin; and 2) inclusions irregular in shape, occasionally showing necking phenomena, occur along the planes crosscutting quartz grains, suggesting their secondary origin. Small-sized (< 6 μm) type Ib inclusions which occur as both primary and secondary inclusions in stage II cacite do not contain CO_2, and are interpreted to be simple H_2O-NaCl types. Any daughter minerals were not observed in any inclusions.

Fig. 3. Photomicrographs showing the various types of fluid inclusions from the Seolhwa gold mine. Scale bars are 10 μm.

Type II inclusions: They consist of two phases at room temperatures showing more than 70 vol.% vapor of the inclusions and a rare visible liquid. These inclusions homogenize to the vapor phase and occur only as primary inclusions in stage I quartz.

Type IV inclusions: These inclusions consist of three (liquid water, CO_2-rich liquid and vapor) phases at room temperature. Their volumetric proportions of carbonaceous phases (liquid + vapor) at 25°C are from 30 to 80 percent (avg = 62%). The whole range of carbonaceous-phase volumetric proportions has been observed within individual samples, which is thought to be a result of fluid unmixing. However, some inclusions having nearly constant phase ratios often form inclusion clusters, suggesting an entrapment of a homogeneous fluid.

Type IV inclusions occur as follows: (1) small groups usually consisting of negative crystals that are relatively isolated and exhibit no planar orientations, (2) isolated, randomly distributed inclusions that are contained in the negative-shaped, subrounded, or irregular vacuoles, and (3) trails of small-sized (< 6 μm) inclusions which represent healed fractures, and these trails occasionally continue to quartz veinlets containing sphalerite and gold. Based on the classification scheme of Roedder (1981, 1984), modes (1) and (2) are primary and mode (3) is secondary or pseudosecondary.

In summary, types II and IV inclusions do not show only fracture control, contrary to type Ib inclusions. Some of the types Ia and II inclusions appear to be pseudosecondary. However, it was difficult to establish a consistent fluid inclusion chronology because repeated fracturing and healing both during and after quartz deposition frequently prevented distinguishing among primary, pseudosecondary, and secondary inclusions using normal criteria (Roedder, 1972, 1981). Therefore, a more practical distinction between primary and pseudosecondary inclusions, and obvious secondary inclusions were employed in this study.

Heating and Freezing Data

A total of 618 fluid inclusions (565 primary + pseudosecondary and 13 secondary inclusions in stage I vein quartz, 29 primary+pseudosecondary and 11 secondary inclusions in stage II calcite) were examined from the Seolhwa gold deposit. Salinity data were reported based on freezing-point depression in the system H_2O-NaCl (Potter *et al.*, 1978) for H_2O-rich, type Ib and II, and on clathrate melting temperatures (Bozzo *et al.*, 1975; Collins, 1979) for CO_2-bearing, type Ia and IV inclusions.

Primary and pseudosecondary inclusions in stage I milky quartz include CO_2-bearing, type Ia and IV inclusions. The wide range of fluid inclusion homogenization temperatures in vein quartz reflects several hydrothermal episodes rather than one specific event, which is indicated by textural evidence of multiple opening and filling of the veins. The results of microthermometric analyses are as follows (Fig. 4 through 10 and Table 1).

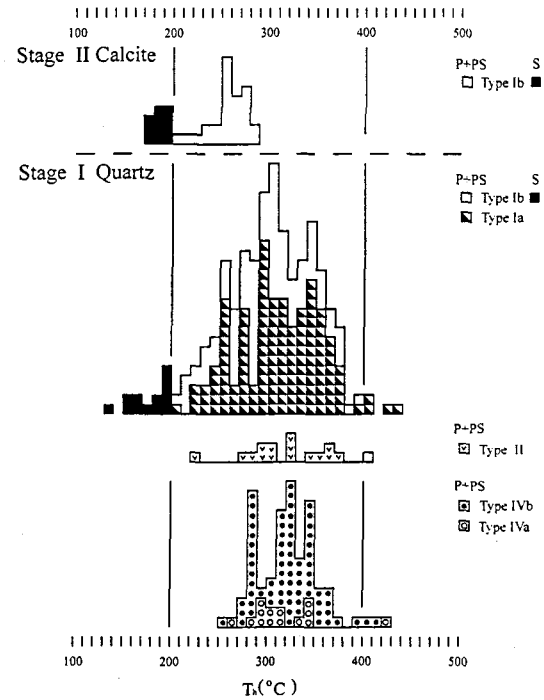

Fig. 4. Frequency diagrams of total homogenization temperature of fluid inclusions in stage I quartz and stage II calcite from the Seolhwa mine.

Table 1. Bulk gas chemistry of the vein quartz from the Seolhwa gold mine.

Sample no.	H_2O (mole%/gr)	CO_2 (mole%/gr)	CH_4 (mole%/gr)	N_2 (mole%/gr)
SH-1	96.97	2.43	0.42	0.18
SH-3	97.18	2.62	0.06	0.14
SH-5	97.00	2.43	0.25	0.31
SH-7	92.41	7.30	0.35	0.06
SH-90	95.77	3.28	0.71	0.24

Type I inclusions: Melting tempertures of the solid CO_2 (Tm-CO_2) in type Ia inclusion range from −61.6° to −56.8°C. Total homogenization temperatures were 226° to 432°C for type Ia inclusions (Fig. 4). Clathrate melting temperatures of type Ia inclusions ranged from 0.1° to 10.0°C. The measured clathrate melting temperatures correspond to salinities ranging from 0.0 to 15.42 wt.% eq. NaCl

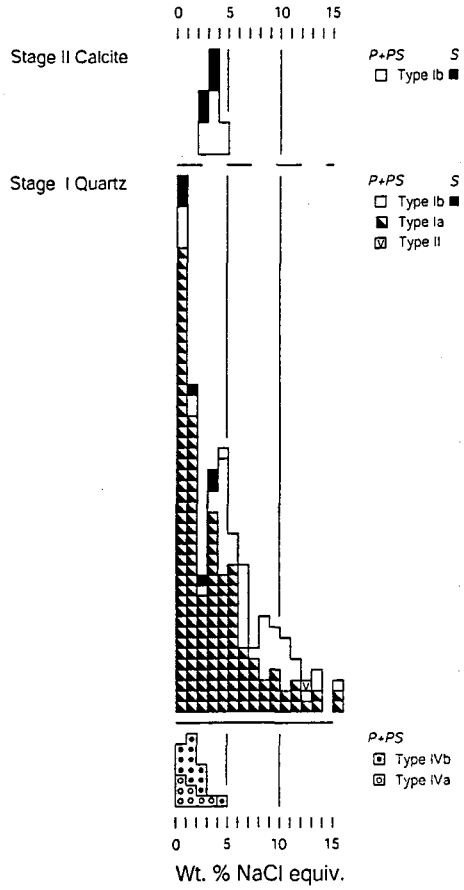

Fig. 5. Frequency diagrams of salinities of fluid inclusions in stage I quartz and stage II calcite from the Seolhwa mine.

(Fig. 5). Type Ib inclusions have inability to nucleate a clathrate on cooling, suggesting the maximum presence of < 2.7 wt.% CO_2 (Hedenquist and Henley, 1985). They homogenized at clearly lower temperatures ranging from 138to 388, and have salinities of 0.18 to 15.17 wt.% eq. NaCl (Figs. 4 and 5).

Homogenization temperatures of primary and pseudosecondary inclusions (type Ib) in stage II calcite range from 171° to 284°C (Fig. 4), which are lower than those of primary and pseudosecondary inclusions in stage I quartz. This may indicate that stage II mineralization occurred from much cooler fluids possibly as a result of much influx of local meteoric waters in the auriferous hydrothermal system. Estimated salinities of stage II fluids range from 2.4 to 4.8 wt.% eq. NaCl (Fig. 5).

Type II inclusions: Most type II inclusions were not suitable for freezing experiments due to their small size. Type II inclusions were homogenized to vapor phase at 224° to 406°C (Fig. 4). Two measured final ice melting tempertures were –3.0° and –9.1°C, indicating total salinities of 4.96 and 12.96 wt.% eq. NaCl (Fig. 5) if neglect the probable clathrate formation by which the ice melting points can be depressed to some degrees (Hendel and Hollister, 1981).

Type IV inclusions: Melting of the solid CO_2 ($Tm\text{-}CO_2$) occurred at temperatures ranging from –59.0° to –56.6°C (type IVa, –59.0° to –56.7°C; type IVb, –58.9° to –56.6°C). Homogenization of carbonaceous phase ($Th\text{-}CO_2$) occurred at following temperatures: type IVa, 15.1° to 26.6°C and type IVb, 16.1° to 30.4°C. Clathrate melting temperature of type IV inclusions could be determined by the sudden appearance of a CO_2-rich liquid which was distorted and blocked from view by the clathrate (Collins, 1979). They ranged from 7.5° to 9.8°C, which are lower than pure CO_2 clathrate melting at 10.0°C (Bozzo *et al.*, 1975). The measured clathrate melting temperatures correspond to salinities ranging from 0.4 to 4.9 wt.% eq. NaCl (Fig. 5). Although type IV inclusions were easily decrepitated prior to total homogenization. 88 total homogenization temperatures were recorded. In cases that the decrepitation occurred before anticipated homogenization, the decrepitation temperatures were used as minimum homogenization temperatures. They include 269° to 429°C for type IVa inclusions (to the aqueous phase) and 253° to 414°C for type IVb (to the carbonaceous phase) (Fig. 4).

Fluid Composition

Bulk gas analyses: Gas compositions of auriferous hydrothermal fluids at Seolhwa gold mine consist mostly of H_2O and CO_2 with the minute amounts of noncondensible gases such as CH_4 and N_2. The gold deposition depends strongly on the con-

stituent gas species in fluids because the chemistry of solubility and/or precipitation mechanism of metallic ions corresponds to the fluid compositions. Analyses on fluid inclusions were executed by the Department of Mineral Development Engineering, University of Tokyo in Japan. In this study, four principal gases (H_2O, CO_2, CH_4, N_2) in each sample were chosen to anlayze on a single ion monitoring mode which is more sensitive. CH_4 and N_2 exist in small amounts (less than 1 mole%). The amounts of H_2O, CO_2, N_2 and CH_4 released from fluid inclusions in the Seolhwa gold mine area are shown in Table 1. The results may show that auriferous hydrothermal fluids consist dominantly of H_2O and CO_2, but rare amounts of CH_4 were also detected on the sample showing variable concentrations. The observed chemistry of hydrothermal fluids for the Seolhwa mine area is similar to those of other Korean Au-Ag deposits (Kim and Cheong, 1999, Fig. 6).

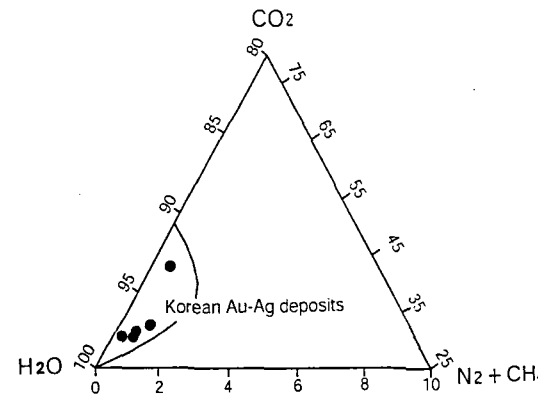

Fig. 6. Triangular plot CO_2-H_2O-N_2 plots of fluid inclusions extracted from quartz. Analysis by gas chromatography. Enclosed area shows the range of Korean Au-Ag deposits.

Initial fluid inclusion: Bulk compositions and densities of type IV inclusions were estimated from data on visual volumes combined with the compositional data and densities of the carbonaceous and aqueous phases of type IV inclusions. Estimation of relative volumes of the carbonaceous and aqueous phases was done by measuring inclusions with a graduated ocular and by assuming that volume was proportional to area, although this method is subject to the uncertainties arising from measuring phase volumes and ignoring the solubility of CO_2 in aqueous part (Roedder, 1984). The quantitative

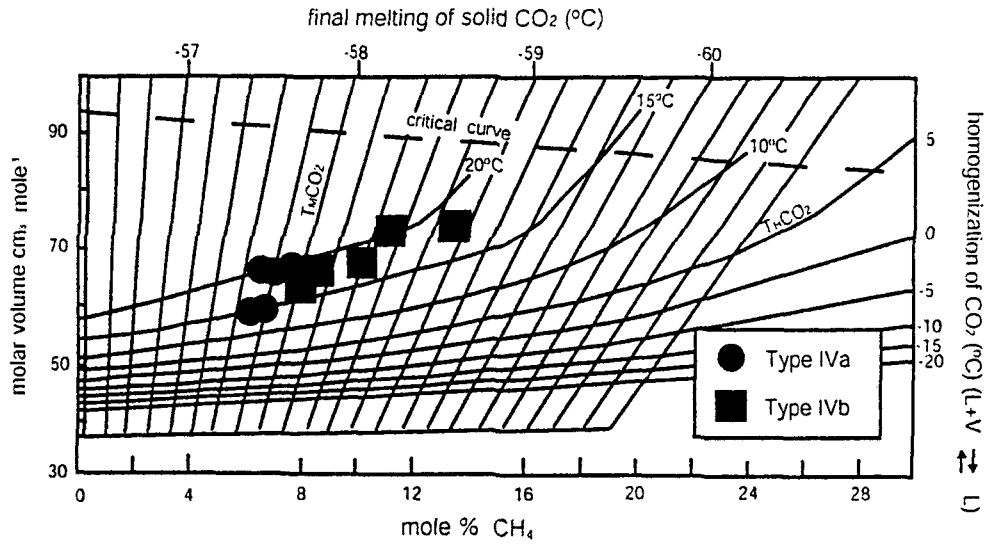

Fig. 7. Graph for calculating the mole composition of CO_2-CH_4 mixtures using the final melting temperature of solid CO_2 (T_MCO_2) and the temperature of liquid-vapour homogenization (T_HCO_2). Solid curves are for T_HCO_2, light curves are for T_MCO_2. The mole% CH_4 is given by the intersection of the appropriate T_HCO_2 and T_MCO_2 curves. This diagram refers to inclusions which homogenize into the liquid state.

V-X_{CH4} projection of the CO_2-CH_4 system (Heyen *et al.*, 1982), combined with the CO_2 melting and homogenization temperatures, was used to estimate the CH_4 contents in type IV inclusions. The estimated mole percent of CH_4 in the nonaqueous part of type IV inclusions are 5 to 14 mole% (type IVa, 5 to 8 mole% and type IVb, 8 to 14 mole%) (Fig. 7). CH_4 is supposed to be the sole agent responsible for the observed CO_2 melting and homogenization temperature depressions. This assumption is likely because the P-V-T-X properties of the coexisting carbonaceous liquid and vapor for CO_2-CH_4-N_2 mixtures containing relatively small amounts of N_2 are very similar with those of the CO_2-CH_4 system between –20° and +15°C (Arai *et al.*, 1971; Sarashina *et al.*, 1971).

Thermal and Compositional Evolution of Hydrothermal Fluids

Wide range of homogenization temperature (~ 200° to ~ 450°C; Fig. 8) of fluid inclusions in vein minerals from the Seolhwa gold mine probably reflects several hydrothermal episodes rather than one specific event. The upper limit of homogenization temperatures is about 450°C for stage I mineralization. Combined with the abundance of liquid CO_2-bearing fluid inclusions, high temperatures for hydrothermal fluids may indicate that the vein mineralization at Seolhwa belongs to mesothermal-hypothermal type deposits.

As described previously, auriferous hydrothermal fluids principally observed in stage I minerals are composed of two types: (1) dominantly aqueous fluids of moderate salinity containing minor amounts of CO_2 (type Ib and Ia), and (2) mixed CO_2-H_2O fluids of low salinity (type IV). CO_2 contents of type IV fluid inclusions are highly variable within individual samples. The CO_2-rich type IV inclusions homogenized at nearly the same temperatures as H_2O-rich type IV inclusions. These observations may indicate that type IV fluid inclusions represent the trapping of immiscible H_2O-CO_2 fluids which evolved through CO_2 effervescence. The relationship between homogenization temperature and salinity for gold-depositing stage I fluids is shown in Fig. 8. Liquid CO_2-bearing type IV inclusions in stage I quartz show a decreasing salinity (from ~ 5 to 0 wt.% NaCl) with decreasing temperature from

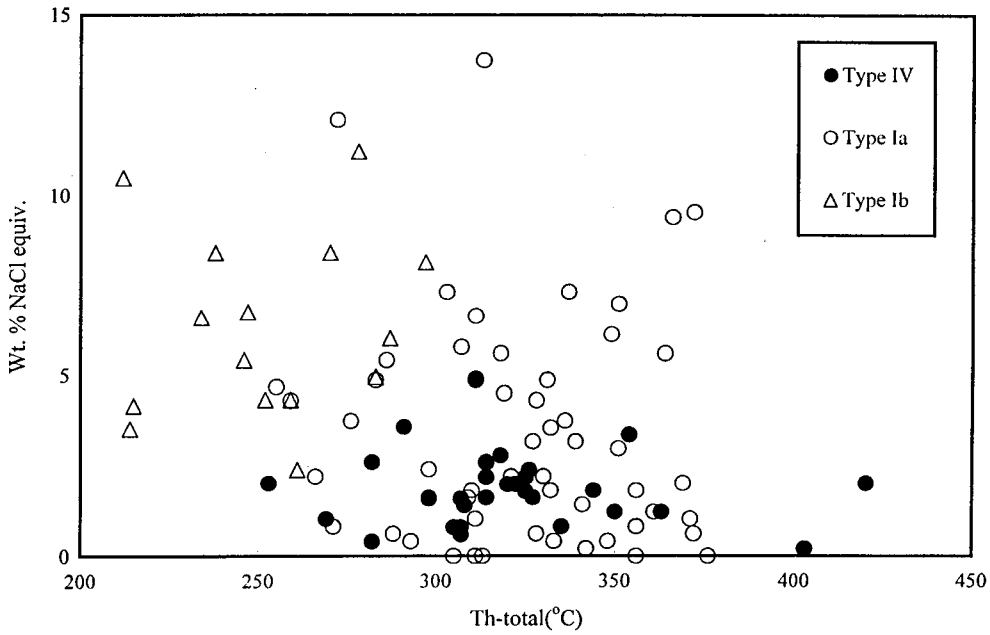

Fig. 8. Homogenization temperature versus salinity diagram for fluid inclusions from the stage I quartz from the Seolhwa mine.

450° to 250°C. This trend is explained by the boiling (CO_2 effervescence) of CO_2-rich fluids, although this trend also may result from simple cooling (Hedenquist and Henley, 1985). The CO_2-poor fluids which had remained after extensive escape of CO_2 gas were probably trapped at temperatures between 370° and 250°C (Fig. 8) as CO_2 clathrate-forming type Ia inclusions in stage I quartz. Type Ia inclusions tend to show an increasing salinity (from < 2 to 15 wt.% eq. NaCl) with decreasing temperature, likely indicating the extensive continued boiling of CO_2-poor fluids. Such continued boiling of auriferous hydrothermal fluids is thought to be the result of pressure decrease during the ascent of hydrothermal fluids. Following the complete loss of CO_2 from stage I fluids, the residual fluids were trapped as CO_2-absent type Ib fluid inclusions (Th °C = 200° ~ 300°C, Fig. 8) in quartz.

Fluid boiling accompanying CO_2 effervescence in auriferous hydrothermal systems may result in abrupt chemical changes in the residual liquid (e.g., f_{O2}, f_{S2}, pH, H_2S, etc.). These changes favor deposition of precious metals through destabilization of metal complexes (Seward, 1973, 1984; Drummond and Ohmoto, 1985; Cole and Drummond, 1986). Gold precipitation mechanisms involving gold bisulfide complex include a decrease in temperature at constant pH, oxidation of the complex, pH decrease, and decrease of sulfur activity by sulfide precipitation and/or H_2S loss accompanying boiling. Several of these possibilities are illustrated by the reaction: $Au(HS)^-_2 + 1/2\ H_{2(g)} + H^+ = Au^0 + 2H_2S_{(aq)}$. Given the frequent association of galena, sphalerite and chalcopyrite with gold in the Seolhwa mine, the role of sulfide precipitation accompanying boiling is critical. Decrease of sulfur activity accompanying boiling, through sulfide deposition and/or H_2S loss, is likely the most important mechanism for gold deposition in the mesothermal-type vein deposits at Seolhwa.

Pressure Consideration

The densities of the carbonaceous phase ($\rho_{carb.}$) were determined from the carbonaceous-phase homogenization temperatures using the phase diagram for CO_2 (Angus *et al.*, 1973; Hollister, 1981) and the isothermal ρ-P diagram for CO_2 at 40°C (Burruss, 1981b). The density of CO_2 for type IVa and IVb are 0.71 to 0.82 g/cc, 0.60 to 0.82 g/cc, respectively. Isochores for type IV fluids (ρ = 0.60 to 0.82 g/cc) intersect the temperature planes of 253 to 326°C (taken from the homogenization temperatures of type IV inclusions, Fig. 4) at pressures of 0.7 to 1.5 kbars (Kennedy, 1954) (Fig. 9). The density of the aqueous phase of type IV inclusions was esimated using the equation of Bodnar (1983). Bulk densities (ρ_{total}) of the selected carbonaceous inclusions were calculated from the estimated densities and volumes of the carbonaceous and aqueous phases. The estimated bulk densities of the inclusions ranged from 0.63 to 0.79 g/cc. Bulk compositions were calculated from data of the densities, volumes and bulk compositions of the carbonaceous and aqueous phases. The calculated mole fraction of the carbonaceous species (X_{CO2}) for type IVa and IVb are 0.16 to 0.62, 0.30 to 0.61, respectively. Based on the calculated fluid composition and estimated fluid trapping temperatures, several immiscibility P-T-X curves for the system H_2O-CO_2-NaCl (Bowers and

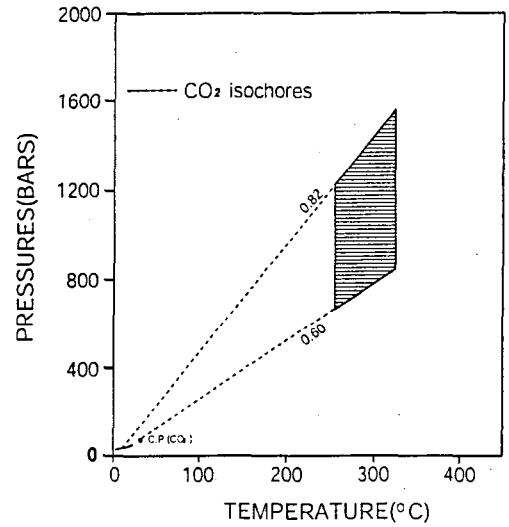

Fig. 9. P-T diagram for the CO_2 system. Data from Kennedy (1954).

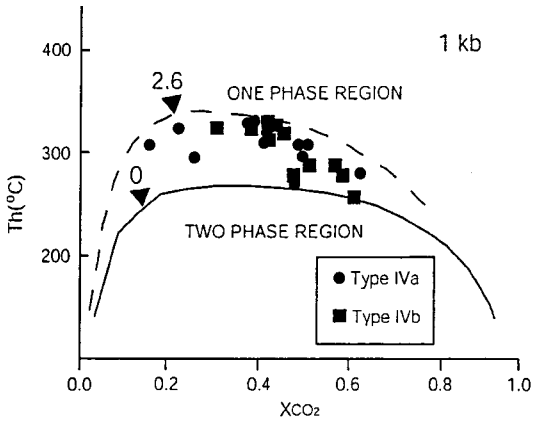

Fig. 10. Total homogenization temperature versus calculated mole fraction of CO_2 for type IV fluid inclusion. The curve delimit the two-phase regions in the CO_2-H_2O-2.6 wt.% NaCl system at 1 kbars. Diagrams after data from Hendel and Hollister (1981) and Bowers and Helgeson (1983a and 1983b).

Helgeson, 1983a, 1983b) were chosen to estimate the trapping pressures of the fluids. We assume maximum pressures did not exceed about 3 kbar based on depth of emplacement estimates of the Jurassic Daebo granites (Cho and Kwon, 1994) that are interpreted to relate to the vein-forming events. The CO_2-H_2O inclusions in stage I quartz plot around the H_2O-CO_2-2.6 wt.% NaCl solvus at 1 kbar (Hendel and Hollister, 1981, Fig. 10). In fact, the average salinities of CO_2-H_2O inclusions in stage I quartz are 2.0 wt.% NaCl. The trapping pressures will be, therefore, slightly lower than 1.0 kbar.

Implication of the Occurrence of Fluid Inclusions with Gold Mineralization

As described in the previous section, gold grains at the Seolhwa deposit occur within randomly-oriented fractures. Such a late mineralization of gold in the history of veining can be correlated with the hydrothermal fluids trapped in the vein quartz as pseudosecondary and/or secondary fluid inclusions. Some of types Ia and IV inclusions occur along healed fractures which somtimes continue to gold-containing veinlets, suggesting both their pseudosecondary origin and therefore their intimate connection with gold mineralization. The fact that the type Ib inclusions usually crosscut the pseudosecondary healed fractures may indicate that type Ib inclusion fluids have not been related with gold deposition.

Some pseudosecondary type Ia inclusions which occur along the healed fractures continuing to the gold-bearing quartz veinlets homogenized at 226 to 432°C (N = 174, avg. = 309). Therefore, the temperatures of the type Ia inclusion fluids are thought to have been related to gold mineralization at Seolhwa indicating mesothermal conditions of gold deposition, which are compared with most epithermal gold deposits (Nash, 1972; Roedder, 1984).

SULFUR ISOTOPE STUDY

Previous studies have shown the utility of stable isotopes in elucidating the origin and history of auriferous hydrothermal fluids in vein-type Au-Ag deposits (Ohmoto, 1972; Taylor, 1973). In this study, sulfur isotope compositions of nine sulfides (3 chalcopyrite, 1 galena, 3 pyrrhotite and 2 sphalerite) were measured in the Seolhwa gold mine district. Standard techniques of extraction and analysis were used, as described by Grinenko (1962). Data are reported in standard notation relative to the Canyon Diablo troilite (CDT) standard for S. The standard error of each analysis is approximately ±0.1 per mil for S. The ^{d34}S values of sulfide minerals in stage I from Seolhwa are as follows (Table 2): pyrrhotite –0.4 to 0.9‰, chalcopyrite 0.2 to 0.8‰, sphalerite 1.1 to 1.4‰, galena –0.6‰. Assuming depositional temperature based on fluid inclusions and paragenetic constraints, the following $\delta^{34}S$ value of H_2S of fluids are calculated (Ohmoto and Rye, 1979; Field and Fifarek, 1985): chalcopyrite 0.3 to 0.9‰, sphalerite 0.8 to 1.1‰, galena 1.1‰ (Table 2). The predominance of pyrrhotite and the alteration assemblage sericite ± kaolinite may indicate that sulfur in the Seolhwa auriferous hydrothermal fluids was dominantly H_2S. Therefore, the $\delta^{34}S_{H2S}$ value of 0.3 to 1.1 (avg. = 0.8) per mil is a good

Table 2. Sulfur isotope data of vein sulfides from the Seolhwa gold mine.

Sample no.	Stage	Mineral	$\delta^{34}S$ (‰)	$\Delta^{34}S$ (‰)	T (°C)[2)]	$\delta^{34}S_{H_2S}$ (‰)[3)]
SH-1	I(M)	Po	0.1			
SH-2	I(M)	Po	−0.4			
SH-3	I(L)	Cp	0.2		300	0.3
SH-5	I(M)	Cp	0.8		340	0.9
SH-7A	I(M)	Sp	1.1		340	0.8
SH-7B	I(M)	Cp	0.5		340	0.6
SH-9A	I(M)	Sp	1.4	Sp-Gn	340	1.1
SH-9B	I(M)	Gn	−0.6	2.0(330±50)[1)]	340	1.1
SH-11	I(M)	Po	0.9			

[1)]Number in parenthesis is sulfur isotope temperature calculated using the equation in Ohmoto and Rye (1979).
[2)]Based on fluid inclusion and/or sulfur isotope temperatures and paragenetic constraints.
[3)]Calculated sulfur isotope compositions of H_2S in ore fluids, using the isotope fractionation equation in Ohmoto and Rye (1979).
Abbreviations: Po = pyrrhotite, Cp = chalcopyrite, Sp = sphalerite, Gn = galena.

approximation of the $\delta^{34}S_{\Sigma S}$ values of the fluids, indicating the derivation of sulfur mainly from an igneous source.

CONCLUSIONS

1. Mesothermal gold mineralization of the Seolhwa mine was deposited in a single stage of massive quartz veins which filled the mainly NE-trending fault shear zones exclusively in the granitoid within the Gyeonggi Massif.

2. The mineralogy of the mesothermal-type veins is simple and consists mainly of rare sulfides and gold. Gold grains (electrum and native gold) associated with sulfides typically occur within the veinlets cutting earlier-deposited quartz. The electrums from the Seolhwa deposit are gold-rich, ranging from 69.7 to 90.9 atom.% Au. The dominant iron-bearing sulfides are pyrrhotite, chalcopyrite and sphalerite, and characteristically contains Bi (-Te-S) minerals.

3. Three main types of fluid inclusions are identified within vein quartz from the Seolhwa mesothermal gold deposit: 1) low-salinity(< 5 wt.% NaCl), liquid CO_2-bearing type IV inclusion, 2) gas-rich (> 70 vol.%), vapor-homogenizing type II inclusion, and 3) aqueous type I inclusions (0 ~ 15 wt.% NaCl) containing small amounts of CO_2. The mesothermal fluids evolved from early carbonaceous (CO_2-CH_4-bearing) to late aqueous fluids with time, due to extensive fluid unmixing (CO_2-CH_4-effervescence). Homogenization temperatures of the early carbonaceous fluids range from 430° to 250°C. Microthermometric data of the carbonaceous fluid inclusions may indicate the presence of minor amounts of CH_4 in inclusion fluids.

4. Initial original fluids of the Seolhwa mesothermal deposits are interpreted to have been homogeneous containing H_2O-CO_2-CH_4-N_2-NaCl components and the following properties: the initital temperature of > 250° to 430°C, X_{CO2} of 0.16 to 0.62, 5 to 14 mole% CH_4, 0.06 to 0.31 mole% N_2 and salinities of 0.4 to 4.9 wt.% NaCl. The auriferous mesothermal fluid have been progressively evolved through extensive fluid unmixing due to the decrease in temperature and pressure, which hase been successively followed by later cooling and dilution of fluids.

5. Pressure-depth consideration may imply that the Seolhwa mesothermal-type gold deposit was formed at pressures of 1.0 kbars. They correspond to mineralization depths of > 3.7 and 10 km, assuming lithostatic and hydrostatic pressure regimes.

6. The $\delta^{34}S$ values of sulfides in the Seolhwa mesothermal gold deposits range from −0.6 to 1.4 per mil, yielding the $\delta^{34}S_S$ values of 0.3 to 1.1 (average 0.8‰) per mil.

ACKNOWLEDGEMENTS

This research was financially supported by the Center for Mineral Resources Research, Korea University and by the academic research fund of Korea University Post-Doc. Grant in 2001 year.

REFERENCES

Angus, S., Armstrong, B., de Reuk, K.M., Altunin, V.V.,

Gadetskii, O.G., Ghapala, G.A., and Rowlison, J.S., 1973, International Thermodynamic Tables of the Fluid State: Carbon Dioxide. New York, Pergamon Press, 386 p.

Arai, Y., Kaminishi, G. and Saito, S., 1971, The experimental determination of the P-V-T-X relations for the carbon dioxide-nitrogen and the carbon dioxide-methane systems. Journal of Chemical Engineering of Japan, 4, 113–122.

Bodnar, R.J., 1983, A method of calculating fluid inclusion volumes based on vapor bubble diameters and P-V-T-X properties of inclusion fluids. Economic Geology, 78, 535–542.

Bowers, T.S. and Helgeson, H.C., 1983a, Calculation of the thermodynamic and geochemical consequences of nonideal mixing in the system H_2O-CO_2-NaCl on phase relations in geologic systems: Equation of state for H_2O-CO_2-NaCl fluids at high pressures and temperatures. Geochimica et Cosmochimica Acta, 47, 1247–1275.

Bowers, T.S. and Helgeson, H.C., 1983b, Calculation of the thermodynamic and geochemical consequences of nonideal mixing in the system H_2O-CO_2-NaCl on phase relations in geologic system: Metamorphic equilibria at high pressures and temperatures. American Mineralogist, 68, 1059–1075.

Bozzo, A.T., Chen, H.S., Kaas, J.R., and Barduhn, A.J., 1975, The properties of hydrates of chlorine and carbon dioxide. Desalination, 16, 303–320.

Burruss, R.C., 1981b, Analysis of phase equilibria in C-O-H-S fluid inclusions. Mineralogical Association of Canadian Short Course Handbook, 39–74.

Cho, D.L. and Kwon, S.T., 1994, Hornblende geobarometry of the Mesozoic granitoids in South Korea and the evolution of the crustal thickness. Journal of Geological Society of Korea, 30(1), 41–61.

Cole, D.R. and Drummond, S.E., 1986, The effect of transport and boiling on Au/Ag ratios in hydrothermal solutions: A preliminary assessment and possible implications for the formation of epithermal precious-metal ore deposits. Journal of Geochemical Exploration, 25, 45–79.

Collins, P.L.F., 1979, Gas hydrates in CO_2-bearing fluid inclusions and the use of freezing data for estimation of salinity. Economic Geology, 74, 1435–1444.

Drummond, S.E. and Ohmoto, H., 1985, Chemical evolution and mineral deposition in boiling hydrothermal systems. Economic Geology, 80, 126–147.

Field, C.W. and Fifarek, R.H., 1985, Light stable-isotope systematics in the epithermal environment. Reviews in Economic Geology, 2, 99–128.

Grinenko, V.A., 1962, Preparation of sulfur dioxide for isotopic analysis. Zeitschrift fur Neorganische Chemie, 7, 2478–2483.

Haynes, F.M., 1985, Determination of fluid inclusion compositions by sequential freezing. Economic Geology, 80, 1436–1439.

Hendel, E.M. and Hollister, L.S., 1981, An empirical solvus for CO_2-H_2O-2.6 wt.% salt. Geochimica et Cosmochimica Acta, 45, 225–228.

Hedenquist, J.W. and Henley, R.W., 1985, The importance of CO_2 on freezing point measurements of fluid inclusions: Evidence from active geothermal systems and implications for epithermal ore deposition. Economic Geology. 80, 1379–1406.

Heo, C.H., Yun, S.T., So, C.S., and Choi, S.G., 2001, Chemical composition and deposition conditions of gold from the Seolhwa mine. Journal of the Korean Institute of Mineral and Energy Resources Engineers, 38, 102–115.

Heyen, G., Ramboz, C., and Dubessy., J., 1982, Simulation des equilibres de phases dans le systeme CO_2-CH_4 en dessous de 50°C et de 100 bars. Application aux inclusions fluides. l'Academie des Sciences Comptes Rendus [Paris], 294, serie II, 203–206.

Hollister, L.S., 1981, Information intrinsically available from fluid inclusions. Mineralogical Association of Canada Short Course Handbook, 6, 1–12.

Kennedy, G.C., 1954, Pressure-volume-temperature relations in CO_2 at elevated temperatures and pressures. American Journal of Science, 252, 225– 241.

Kim, K.H. and Cheong, H.R., 1999, Gas and solute compositions of fluid inclusions in quartz from some base-metal ore deposits, South Korea. Economic and Environmental Geology, 32, 421–434.

KORES, 1983, A report on the amount of reserves of the Seolhwa gold mine, 16 p.

Nash, J.T., 1972, Fluid inclusion studies of some gold deposits in Nevada. U.S. Geological Survey Professional Paper 800-C, 15 19.

Ohmoto, H., 1972, Systematics of sulfur and carbon isotopes in hydrothermal ore deposits. Economic Geology, 67, 551–578.

Ohmoto, H. and Rye, R.O., 1979, Isotopes of sulfur and carbon, in Barnes, H.L., ed., Geochemistry of hydrothermal ore deposits. New York, Wiley Interscience, 509–567.

Potter, R.W., III, Clynne, M.A., and Brown, K.L., 1978, Freezing point depression of aqueous sodium chloride solutions. Economic Geology, 73, 284–285.

Roedder, E., 1972, The composition of fluid inclusions. United States Geological Survey Professional Paper 440JJ, 164 p.

Roedder, E., 1981, Origin of fluid inclusions and changes that occur after trapping. Minerlogical Association of Canada Short Course Handbook 6, 101–137.

Roedder, E., 1984, Fluid inclusions. Review in Mineral-

ogy, 12, 644 p.

Sarashina, E., Arai, Y., and Saito, S., 1971, Vapor-liquid equilibria for the nitrogen-methane-carbon dioxide system. Journal of Chemical Engineering of Japan, 4, 377–378.

Seward, T.M., 1973, Thio complexes of gold and the transport of gold in hydrothermal ore solutions. Geochimica et Cosmochimica Acta, 37, 337–399.

Shelton, K.L., So, C.S., and Chang, J.S., 1988, Gold-rich mesothermal vein deposits of the Republic of Korea: Geochemical studies of the Jungwon gold mine area. Economic Geology, 83, 1221–1237.

Shepherd, T.J., Rankin, A.H., and Alderton, D.H.M., 1985, A practical guide to fluid inclusion studies. Blackie & Sons Ltd. 239 p.

Shimazaki, H., Lee, M.S., Tsusue, A., and Kaneda, H., 1986, Three epochs of gold mineralization in South Korea. Mining Geology, 36, 265–272.

Taylor, H.P. Jr., 1973, $^{18}O/^{16}O$ evidence for meteoric-hydrothermal alteration and ore deposition in Tonopah, Comstock Lode, and Goldfield mining districts, Nevada. Economic Geology, 68, 744–764.

2001년 3월 5일 원고 접수
2001년 6월 18일 수정원고 접수
2001년 8월 4일 원고 채택